Proceedings of the 14th Asian Control Conference
July 5-8, 2024, Dalian, China

A Novel Haptic Takeover Method Based on Human-Machine Collaboration States

1st Yunbo Zhao
Department of Automation, University of Science and Technology of China
Hefei, China
Institute of Artificial Intelligence, Hefei Comprehensive National Science Center
Hefei, China
ybzhao@ustc.edu.cn

2nd Zuhao Xie
Department of Automation, University of Science and Technology of China
Hefei, China
zhexie@mail.ustc.edu.cn

3rd Chang Xu
Department of Automation, University of Science and Technology of China
Hefei, China
changxu@mail.ustc.edu.cn

4th Xiuhua Liang
Department of Automation, University of Science and Technology of China
Hefei, China
liangxiuhua@mail.ustc.edu.cn

5th Ruiyu Xia
Department of Automation, University of Science and Technology of China
Hefei, China
ruiyu_xia@163.com

6th Jiayu Li
Department of Automation, University of Science and Technology of China
Hefei, China
jyli_xxy@mail.ustc.edu.cn

***Abstract*—The current stage of autonomous driving calls for drivers to remain actively engaged within the control loop in anticipation of the need for takeover operations. However, regaining control of the vehicle from a state of low situation awareness (SA) poses a challenge. To address this issue, this research introduces a novel takeover method based on haptic shared control, ensuring a smooth and safe takeover process. A symmetric softmax function is formulated to evaluate muscle state, taking into account the varying torque thresholds associated with different vehicle speeds, as well as utilizing the driver's cognitive state to characterize their SA. Within the takeover process, a coordinator leverages the driver's SA and human-machine intention similarity to determine the current state of human-machine collaboration. Subsequently, different control allocation strategies are then adopted for different states, and the driver is guided through force feedback. Experiment results demonstrate the effectiveness of the proposed method, showcasing its ability to facilitate a smooth and safe transfer of control, regardless of the presence of conflicts or the harmonious state existing between the human driver and the automated system.**

***Index Terms*—autonomous driving, haptic shared control, authority transfer, takeover**

I. Introduction

With the rapid advancement of artificial intelligence (AI) technology, autonomous vehicles have witnessed substantial progress in recent years [1]. However, due to technological and regulatory constraints, the majority of autonomous vehicles currently operating on roads are classified at Level 2 and Level 3 (SAE [2]). Nonetheless, at the present stage, human drivers are still mandated to remain within the control loop, with advanced driving assistance system (ADAS) reverting control to the driver when necessary, a process commonly referred to as **takeover** [3], [4].

Despite the requirement for drivers to remain in the control loop, human supervision can be prone to distraction, attention shifts, or engagement in non-driving related task (NDRT), leading to a loss of SA which is detrimental to takeover process [5]–[7]. Even with attentive supervision, takeover events may involve abrupt actions [8]. Such tense and abrupt takeover events would result in vehicle instability or precarious situations, affecting subsequent manual driving. Therefore, this poses a challenge that achieving safe and smooth control takeover in situations where drivers experience a loss of SA.

Currently, the prevalent commercial strategy involves traded control following a Request to Intervene (RTI), demanding immediate driver takeover, even if the driver is in a state of loss of SA. In addition to directly transferring control authority to the human driver, a method of considerable interest is haptic shared control where both human and machine exert external forces on the control interface, facilitating mutual comprehension of intentions through force magnitude and direction [9]. This approach holds promise in smoothing the takeover process and regaining SA to ensure safety [5], [10].

Previous studies treated the takeover process as an optimization problem [11], considered the influence of human torque on control transfer [12], [13], explored various collaboration states and adjusted PID parameters to achieve smooth transition [14], [15], and considered road conditions [16]. However, in the context of takeover, previous studies mainly focused on lateral vehicle control. These studies either entirely adhere to ADAS or human preferences, neglecting conflicts between machine and human preferences which present a challenge in achieving smooth control transition.

This work was supported by the Dreams Foundation of Jianghuai Advance Technology Center (NO.Q/JH-063-2023-T02 A/O). Corresponding author: Yunbo Zhao (e-mail: ybzhao@ustc.edu.cn).

The primary contribution of this study lies in introducing a smooth haptic takeover method based on the states of human-machine collaboration. Instead of adhering to ADAS or human preferences, this method dynamically adjusts control authority based on four collaboration states, ensuring smoothness and safety throughout the takeover process, whether in harmonious or conflicted situations. Additionally, it takes into account both the lateral and longitudinal control of the vehicle, further enhancing safety. The remainder of the paper is structured as follows: Section II elaborates on evaluation of driver's situation awareness. Section III outlines control authority allocation and shows the whole framework of our method. Section IV presents experiment setup and results, and Section V summarizes the entire paper.

II. Evaluation of driver's Situation Awareness

The SA (Q) of drivers may be correlated with their physiological states [17]. To assess a driver's SA, we consider cognitive state (Q_C) and muscle state (Q_T) as important indicators, integrating both according to the method proposed by [3]

$$Q = 1 - e^{-(1+Q_C)^2 \cdot Q_T^3}. \tag{1}$$

A. Evaluation of Driver's Cognitive State

Cognitive load (C) reflects a driver's perception of the environment to some extent, with past research often suggesting that both excessively high and low cognitive load are detrimental to driving task performance. Here, we adopt the method from [3] to describe the relationship between cognitive load and cognitive state:

$$Q_C = Q_{C\max} - 4\left(C - 0.5\right)^2. \tag{2}$$

Here, Q_C represents cognitive state, $Q_{C\max}$ denotes the upper limit of cognitive state. Cognitive load may be influenced by factors such as the driver's physiological state (e.g., heart rate, electromyography signals, eye-tracking data [18]), as well as vehicle status, traffic conditions, among others. We employ the method in [19] for computing cognitive load, which assumes a gradual recovery of cognitive load over time.

B. Evaluation of Driver's Muscle State

In addition to cognitive state, a driver's muscle state also reflects the level of SA. During takeover processes, human torque must meet certain requirements. Relationship between muscle state during takeover and corresponding authority is described as a nonlinear process resembling a softmax function shape in [3], [19]. Simplistically, in a relaxed muscle state, the torque applied to the steering wheel by the driver is low, indicating lower SA, whereas in a tense muscle state, SA is higher. However, this overlooks the tense state of the driver during initial takeover, which may lead to excessive torque applied to the steering wheel. In such cases, using the original method would yield opposite conclusions, potentially leading to hazardous situations.

Therefore, we introduce a torque threshold T_t, where the evaluation of muscle state gradually decreases when the driver's torque exceeds T_t. We design symmetric softmax function with a variable torque threshold parameter to achieve this:

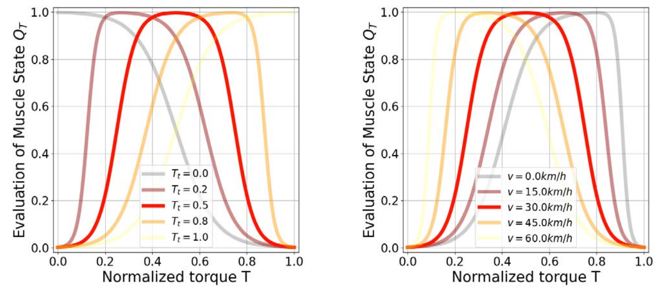

(a) (b)

Fig. 1. (a) The relationship between evaluation of muscle state and torque under different T_t ($a = 12.5, b = 0.5$). (b) The relationship between evaluation of muscle state and torque under different speed v ($c = 3, b = 60$).

$$Q_T = \frac{1}{1+e^{-\frac{a}{T_t}(T - bT_t)}} + \frac{1}{1+e^{-\frac{a}{1-T_t}(T - b(T_t+1))}} - 1, \tag{3}$$

$$T = \frac{T_{\max} - T}{T_{\max}}. \tag{4}$$

Here, Q_T represents the evaluation of the current driver's muscle state, T_{real} denotes the torque applied by the driver, $T_{\max}$ is the maximum torque the driver can apply, a is used to modulate the slope of the curve, while b is used to adjust the position of the curve. As depicted in Fig. 1(a), this function ensures a declining trend for Q_T as it moves away from T_t while maintaining a stable state around T_t.

Furthermore, different steering angles at varying speeds will result in different effects on the vehicle. Generally, higher speeds should entail smaller steering angles and vice versa. Thus, we design a variable torque threshold as $T_t = \frac{v_{\max} - v}{v_{\max}}$, where v represents the current vehicle speed, and $v_{\max}$ represents the maximum vehicle speed. The relationship between muscle state score and torque at different speeds is depicted in Fig. 1(a). It can be observed that when the vehicle speed reaches v_{max}, the curve completely transforms into a softmax function. However, even a slight torque applied at this point leads to rapid score transitions, which is also the case when $v = 0$, which is unreasonable. To mitigate adverse effects at the edge of the speed threshold, we adopt the following torque-speed relationship:

$$T_t = \frac{1}{1+e^{-c(\frac{v_{\max} - v}{v_{\max}} - d)}}. \tag{5}$$

Here, c and d are adjustment parameters for T_t. With this relationship, the evaluation of muscle state and torque under different speeds is depicted in Fig. 1(b).

III. Human-machine interaction design

A. Vehicle System Modeling and Control Authority Allocation

We utilize a 2-degree-of-freedom linear time-varying bicycle model to depict kinematic behavior and design the controller. The overall vehicle system kinematics model is formulated as

$$\dot{\chi} = f(\chi, u). \tag{6}$$

Here, $\chi = \begin{bmatrix} x & y & \varphi \end{bmatrix}^T$, where (x, y) denote the coordinates of the vehicle's rear axle center, and φ represents the vehicle's yaw angle. The input is defined as $u = \begin{bmatrix} v & \delta \end{bmatrix}^T$, where v is the velocity of the vehicle's rear axle, and δ is the steering angle of the front wheels. Given a reference trajectory χ_r, we have: $\dot{\chi}_r = f(\chi_r, u_r)$, where $\chi_r = \begin{bmatrix} x_r & y_r & \varphi_r \end{bmatrix}^T$, $u_r = \begin{bmatrix} v_r & \delta_r \end{bmatrix}^T$.

At the reference trajectory point, perform a Taylor expansion for (6), and neglect higher-order terms, than by discretizing the results with a sampling time T, we obtain

$$\tilde{\chi}(k+1) = A_{k,t}\tilde{\chi}(k) + B_{k,t}\tilde{u}(k), \tag{7}$$

where

$$A_{k,t} = \begin{bmatrix} 1 & 0 & -v_r \sin\varphi_r T \\ 0 & 1 & v_r \cos\varphi_r T \\ 0 & 0 & 1 \end{bmatrix}, \tag{8}$$

$$B_{k,t} = \begin{bmatrix} \cos\varphi_r T & 0 \\ \sin\varphi_r T & 0 \\ \frac{\tan\delta_r T}{l} & \frac{v_r T}{l\cos^2\delta_r} \end{bmatrix}. \tag{9}$$

Here, l represents the wheelbase.

We adopt model predictive control as ADAS's control algorithm. The control outputs can be obtained by solving the following optimization problem:

$$\min_{u(k:k+N_c-1)} \boldsymbol{J}(k), \tag{10a}$$

$$\text{s.t. } \tilde{\chi}(k+1) = A_{k,t}\tilde{\chi}(k) + B_{k,t}\tilde{u}(k), \tag{10b}$$

$$\Delta v_{\min} < \Delta v < \Delta v_{\max}, \tag{10c}$$

$$\Delta \delta_{\min} < \Delta \delta < \Delta \delta_{\max}. \tag{10d}$$

Here, $J(k)$ represents the cost function

$$\begin{aligned} \boldsymbol{J}(k) = \sum_{j=1}^{N_p} & \tilde{\chi}^{\mathrm{T}}(k+j \mid k)\boldsymbol{Q}\tilde{\chi}(k+j \mid k) + \\ & \tilde{u}^{\mathrm{T}}(k+j-1)\boldsymbol{R}\tilde{u}(k+j-1), \end{aligned} \tag{11}$$

where $\boldsymbol{Q}$ and $\boldsymbol{R}$ are the weighting matrices. The first term ensures the controller follows the reference path, while the second penalizes control effort. Constraints (10c) and (10d) are used to restrict control increments, ensuring smooth driving.

To ensure the continuity of human perception of vehicle control during the takeover process and afterwards, a direct haptic shared control approach is employed, integrating inputs from both human and ADAS. Thus, the ultimate control input u^* applied to the vehicle is a combined effect of both:

$$u^* = \alpha u_d + (1-\alpha)u_a. \tag{12}$$

Here, u_d and u_a represent the front wheel steer angles input by the driver and the ADAS respectively, with α denoting the authority allocation coefficient. The relationship between the front wheel steering angle δ and the steer wheel angle ω is described by $\delta = k\omega$, where k represents the scale factor. A PID controller adjusts the torque T_a to align the steering wheel angle with the desired front wheel angle set by the ADAS. The torque outputs from both the driver and the ADAS act together on the steering wheel, with the torque provided by the ADAS decreasing as the authority of the driver increases:

$$T = T_d + (1-\alpha)T_a. \tag{13}$$

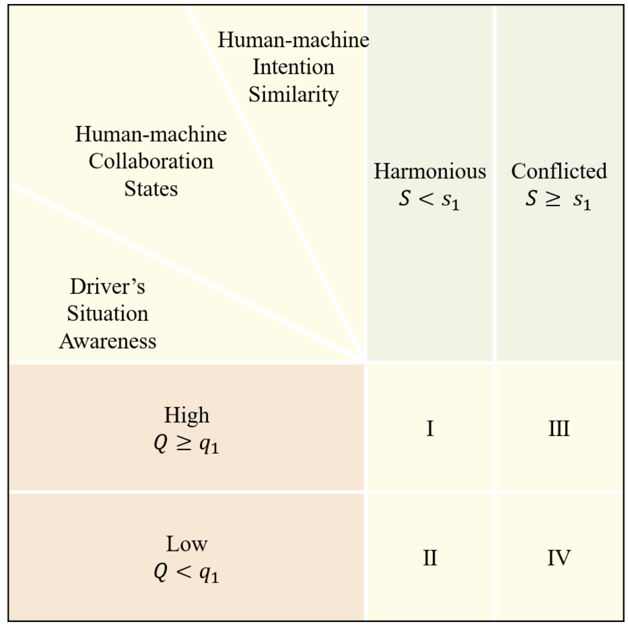

Fig. 2. Four states of human machine collaboration.

B. Evaluation of Human-machine Collaboration States and Transfer of Control Authority

Previous research on the process of takeover has overlooked the conflict of human-machine intentions, particularly manifested in the control of the steering wheel. We introduce a human-machine intention similarity evaluation function, denoted as S, considering the magnitude and direction of torque exerted by both human driver and ADAS, as well as the disparity between the actual positions and the expected positions of the steering wheel by the ADAS:

$$\begin{aligned} S = \omega_1\sqrt{(|T_d| - |T_a|)^2} + \omega_2\sqrt{(D_d - D_a)^2} \\ + \omega_2\sqrt{(P_r - P_a)^2}. \end{aligned} \tag{14}$$

Here, $|T_d|$ and $|T_a|$ represent the magnitude of torque exerted by the driver and the ADAS respectively, D_d and D_a represent the direction of torque exerted by the driver and the ADAS respectively, P_r and P_a represent the actual position of the steering wheel and the expected position by the driver and the ADAS respectively, $\omega_1, \omega_2, \omega_3$ are weighting parameters. Then, we introduce a threshold s_1 for human-machine intention similarity to determine whether the human-machine collaboration state is in harmonious or conflicted. A SA threshold q_1 is introduced to describe the level of driver's SA. Based on this, we categorize the human-machine collaboration

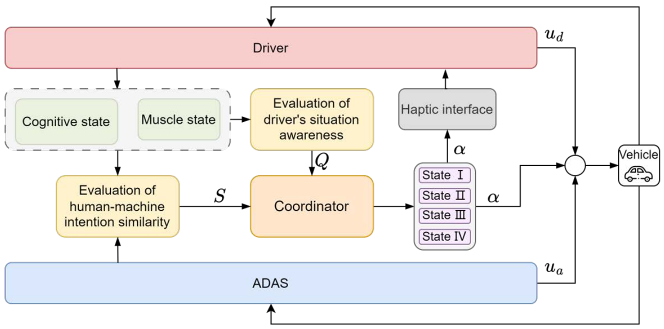

Fig. 3. Framework of smooth haptic takeover method.

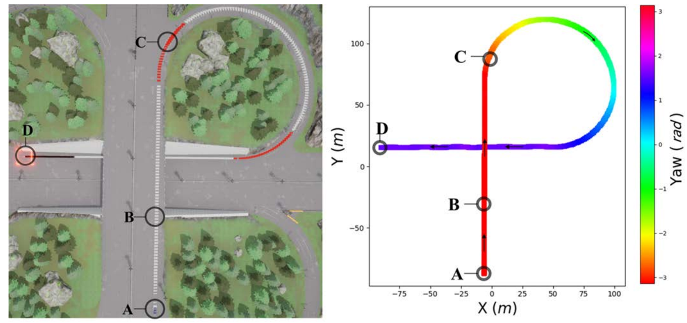

Fig. 4. Overlook of the map(left).Coordinate map with yaw(right).

state into four categories as follows according to the scheme shown in Fig. 2:

- **State I**: Human and machine demonstrate similar intentions, and the driver's SA is high, which is the most harmonious state during the process of takeover. This state represents the smoothest takeover process, thus only requiring a smooth transition of control authority:

$$\alpha = \frac{1}{1 + e^{\eta - \epsilon Q}}. \tag{15}$$

Here, η and ϵ are used to adjust the slope and the position of α respectively.

- **State II**: Human and machine demonstrate similar intentions, but the driver's SA is low. Lateral control authority transition is the same as State 1. However, longitudinal deceleration is applied to provide the driver with more reaction time to ensure safety:

$$v := v - n_1(1 - Q)T. \tag{16}$$

Here, v represents the current speed, T is the sampling time, and n_1 is an adjustment parameter.

- **State III**: Conflict arises between human and machine, yet the driver maintains a high level of SA. In this case, control authority should be quickly restored to the driver to minimize ADAS interference:

$$\alpha = \frac{1}{1 + e^{\eta - \epsilon (Q \cdot S)}}. \tag{17}$$

- **State IV**: Conflict occurs between human and machine when the driver's SA is low. This presents the most challenging scenario in the process of takeover and suggests the possibility of the driver exhibiting exaggerated behaviors due to nervousness. In this scenario, lateral authority transfer should be ceased immediately, and deceleration should be applied promptly to ensure safety:

$$v := v - n_2(1 - Q)T. \tag{18}$$

Here, n_2 is an adjustment parameter.

Throughout the takeover process, a coordinator continuously evaluates the human-machine collaboration states in real-time. The framework of our method is illustrated in Fig. 3.

IV. Experiment and Results

A. Setup

In our experiment, simulations were conducted using the CARLA simulator. We selected a region with a high steering rate as the testing segment (Fig. 4), which mirrors one of the challenges encountered by autonomous vehicles in real-world driving environments. Interaction between the driver and the simulation environment was facilitated through a Logitech G29 steering wheel. Five participants, all possessing driver's licenses, with an average age of 24 years, were involved in the experiment.

Initially, participants were allotted 10 minutes to navigate the simulation environment following a designated route (excluding the test segment) and experience entering and exiting autonomous driving mode to familiarize themselves with the driving equipment and environment. Participants were able to monitor information of simulation environment through a display, as illustrated in Fig. 5. Then, participants commenced formal testing. The test segment, as shown in Fig. 4, required participants to depart from point A, initiate autonomous driving mode at point B (with the vehicle traveling at a constant longitudinal velocity of 15 m/s), and ultimately arrive at point D. Near the approaching bend at point C, the RTI prompt was issued by the ADAS, requiring the driver to assume control of the vehicle. A comparison between our method and direct control authority transition will be presented. The constraint parameters for optimizing are established to ensure the vehicle's smooth motion, a higher weight is assigned to the steering wheel position difference, as this most effectively reflects human-machine intention similarity. The key parameters are outlined in Table I.

B. Result

Each participant undergoes 10 driving experiments on the test route, with 5 experiments employing the method proposed in this paper, and the remaining 5 utilizing traded control. In the traded control scenario, ADAS issues an RTI at point C, with the actual control transition occurring 4 seconds later. If the driver intervenes within this 4-second window, control would be promptly returned to the driver.

Across all experiments, our proposed method results in only 1 accident (vehicle collision with the roadside), whereas traded

Fig. 5. Monitor view of the simulation.

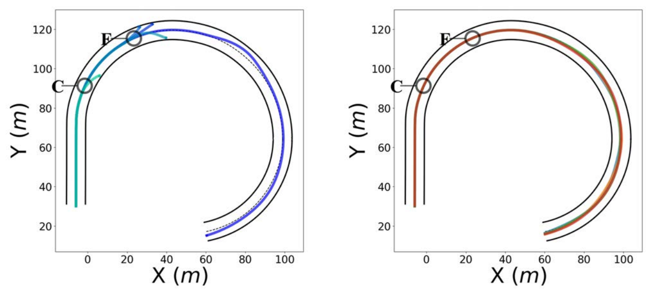

(a) (b)

Fig. 6. (a)Trajectory of traded control method. (b)Trajectory of the proposed method.

control lead to 5 accidents. This indicates a slight advantage of our method over traded control. Fig. 6 illustrates a segment of the trajectories from a portion of the experiments. Accidents in traded control scenarios frequently occur at the moment of RTI issuance, where drivers might react impulsively, such as firmly gripping the steering wheel or oversteering. Additionally, accidents tended to arise upon the return of control to the drivers (approximately at point F), as drivers might overlook the vehicle's self-alignment torque or engage in oversteering.

Our proposed method ensures driving safety amidst human-machine conflict. The process of resolving human-machine conflicts based on our method is delineated in Fig. 7, with the background color denoting the current human-machine collaboration state. Subsequent to RTI issuance, the driver steers the wheel in response to torque exerted by the machine, resulting in a collaboration state of II. Subsequently, due

TABLE I
KEY PARAMETERS

Parameter	Value	Description
$\Delta v_{\min}$	-0.2	minimum decrement of velocity
$\Delta v_{\max}$	0.2	maximum increment of velocity
$\Delta \delta_{\min}$	-0.47(deg)	minimum decrement of wheel steer angle
$\Delta \delta_{\max}$	0.47(deg)	maximum increment of wheel steer angle
l	2.65(m)	wheelbase
$\omega_1/\omega_2/\omega_3$	1/1/20	weighting parameter of S
ϵ/η	5/10	adjustment parameter of α
n_1/n_2	1/3	adjustment parameter of v
T	0.02(s)	sampling time

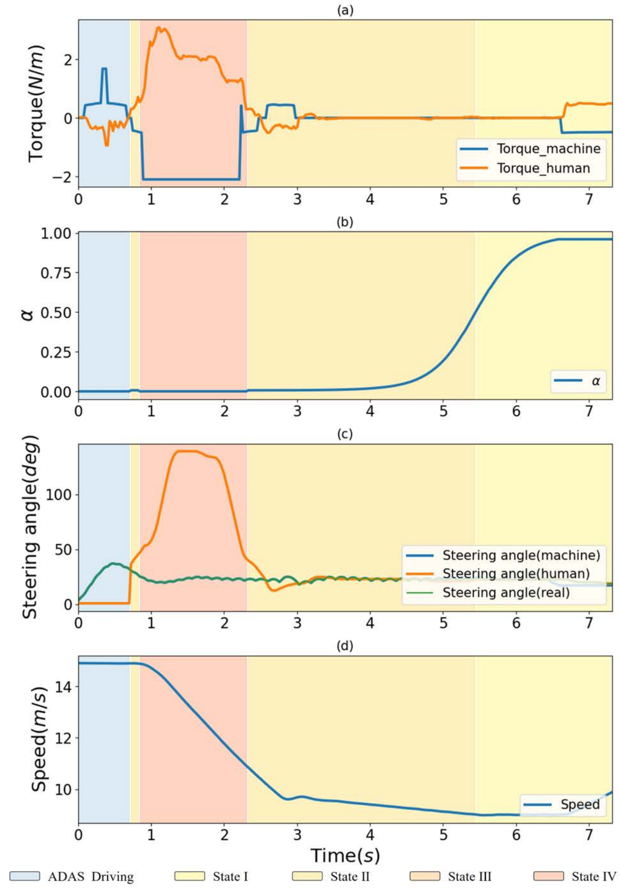

Fig. 7. Process of resolving human-machine conflicts using the proposed method.

to tension, the driver oversteers, engendering a conflict and shifting the collaboration state to IV, thereby prompting the machine to generate reverse torque as a cue for the driver. Throughout this process, the weight allocation coefficient α remains low and constant, thereby yielding an actual steering angle closer to the ADAS output, while the vehicle speed decreases to ensure safety. This underscores that the method proposed in this paper effectively mitigates actions by drivers exhibiting low levels of SA that could compromise vehicle safety.

Guided by torque cues, the driver gradually restores SA, reduces torque, and gradually steers the wheel to the correct position, thereby restoring the human-machine collaboration state to II. The driver's authority gradually increases, slowing the decrease in vehicle speed. As the driver's SA recovers, the human-machine collaboration state transfers to I, with vehicle speed maintained, and control authority gradually transfers to the driver until fully assumed by humans. The entire takeover process takes approximately 6 seconds.

Fig. 8 illustrates the operational mechanism of our method in a harmonious human-machine collaboration scenario. Subsequent to RTI issuance, the driver turns the wheel with assistance, with a delay in the driver's actions but without

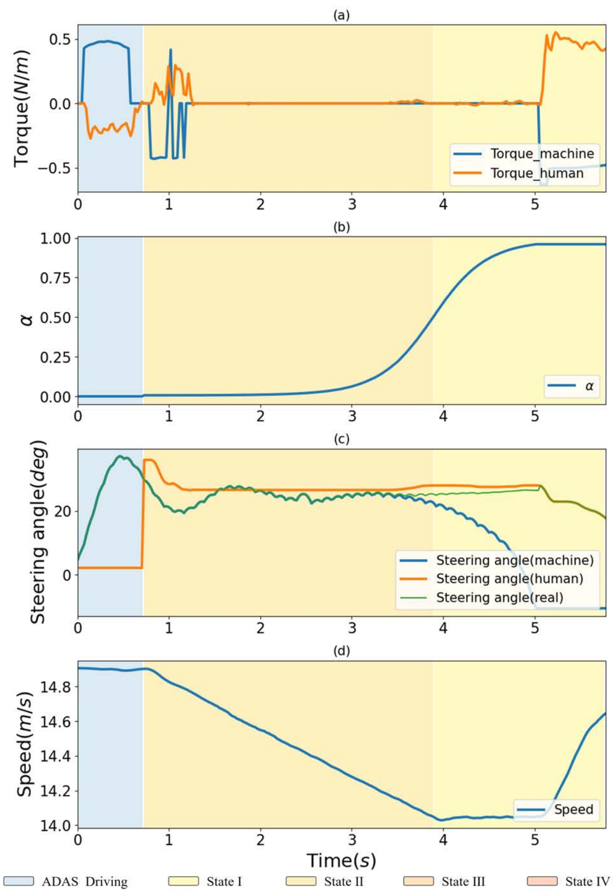

Fig. 8. Operational mechanism of our method in a harmonious human-machine collaboration scenario.

causing conflicts, resulting in a collaboration state of II. Control authority is smoothly transferred to the driver, with a slight decrease in vehicle speed, but slower than in state IV. As the driver's SA improves, the human-machine collaboration transfers to state I, with vehicle speed maintained, and the actual steering wheel angle gradually aligning with the driver's input, thereby effecting a smooth transition of control authority to the driver. The entire transition process spans approximately 4 seconds, shorter than scenarios involving human-machine conflict. In a harmonious human-machine collaboration scenario, the method proposed in this paper could achieve smooth and rapid transitions.

V. Conclusion

This paper introduces a novel takeover method founded on haptic shared control, which aims to facilitate a smooth and safe transition of control authority from ADAS to human drivers within driving contexts. The cognitive and muscle states of the driver are used to describe the driver's SA. During the takeover process, the coordinator determines the human-machine collaboration state based on the driver's SA and human-machine intention similarity, and adopts different control allocation strategies according to different states. The simulation demonstrates the effectiveness of the proposed method to manage human-machine conflicts, ensure safety, and complete authority transitions in a harmonious human-machine collaboration scenario.

References

[1] L. Chen, Y. Li, C. Huang, B. Li, Y. Xing, D. Tian *et al.*, "Milestones in autonomous driving and intelligent vehicles: Survey of surveys," *IEEE Transactions on Intelligent Vehicles*, vol. 8, no. 2, pp. 1046–1056, 2022.

[2] "Taxonomy and Definitions for Terms Related to Driving Automation Systems for On-Road Motor Vehicles - SAE International," https://www.sae.org/standards/content/j3016_202104/.

[3] Z. Zhang, C. Wang, W. Zhao, C. Xu, and G. Chen, "Driving Authority Allocation Strategy Based on Driving Authority Real-Time Allocation Domain," *IEEE Transactions on Intelligent Transportation Systems*, vol. 23, no. 7, pp. 8528–8543, Jul. 2022.

[4] Y. Chen, X. Zhang, and J. Wang, "Robust Vehicle Driver Assistance Control for Handover Scenarios Considering Driving Performances," *IEEE Transactions on Systems, Man, and Cybernetics: Systems*, vol. 51, no. 7, pp. 4160–4170, Jul. 2021.

[5] H. E. B. Russell, L. K. Harbott, I. Nisky, S. Pan, A. M. Okamura, and J. C. Gerdes, "Motor learning affects car-to-driver handover in automated vehicles," *Science Robotics*, vol. 1, no. 1, p. eaah5682, Dec. 2016.

[6] C. Gold, R. Happee, and K. Bengler, "Modeling take-over performance in level 3 conditionally automated vehicles," *Accident Analysis & Prevention*, vol. 116, pp. 3–13, Jul. 2018.

[7] J. C. F. De Winter, S. M. Petermeijer, and D. A. Abbink, "Shared control versus traded control in driving: A debate around automation pitfalls," *Ergonomics*, vol. 66, no. 10, pp. 1494–1520, Oct. 2023.

[8] F. Roche, M. Thüring, and A. K. Trukenbrod, "What happens when drivers of automated vehicles take over control in critical brake situations?" *Accident Analysis & Prevention*, vol. 144, p. 105588, Sep. 2020.

[9] A. D.A. and M. M., "Neuromuscular Analysis as a Guideline in designing Shared Control," in *Advances in Haptics*, M. Hosseini, Ed. InTech, Apr. 2010.

[10] A. Hamdan, R. Talj, and V. Cherfaoui, "Transition Management Between an Autonomous Vehicle and a Real Human Driver, in a Context of Take-Over Request," *IFAC-PapersOnLine*, vol. 55, no. 14, pp. 65–70, 2022.

[11] Y. Jiang, X. Zhang, X. Xu, X. Zhou, and Z. Dong, "Event-triggered shared lateral control for safe-maneuver of intelligent vehicles," *Science China Information Sciences*, vol. 64, no. 7, p. 172203, Jul. 2021.

[12] Y. Li, C. Lv, and J. Xue, "A Novel Predictive Haptic Control Interface for Automation-to-Human Takeover of Automated Vehicles," in *2019 IEEE Intelligent Vehicles Symposium (IV)*. Paris, France: IEEE, Jun. 2019, pp. 994–999.

[13] C. Lv, Y. Li, Y. Xing, C. Huang, D. Cao, Y. Zhao, and Y. Liu, "Human–Machine Collaboration for Automated Driving Using an Intelligent Two-Phase Haptic Interface," *Advanced Intelligent Systems*, vol. 3, no. 4, p. 2000229, Apr. 2021.

[14] T. Wada, K. Sonoda, T. Okasaka, and T. Saito, "Authority transfer method from automated to manual driving via haptic shared control," in *2016 IEEE International Conference on Systems, Man, and Cybernetics (SMC)*, Oct. 2016, pp. 002 659–002 664.

[15] T. Saito, T. Wada, and K. Sonoda, "Control Authority Transfer Method for Automated-to-Manual Driving Via a Shared Authority Mode," *IEEE Transactions on Intelligent Vehicles*, vol. 3, no. 2, pp. 198–207, Jun. 2018.

[16] K. Okada, K. Sonoda, and T. Wada, "Transferring From Automated to Manual Driving When Traversing a Curve via Haptic Shared Control," *IEEE Transactions on Intelligent Vehicles*, vol. 6, no. 2, pp. 266–275, Jun. 2021.

[17] J. C. F. De Winter, Y. B. Eisma, C. D. D. Cabrall, P. A. Hancock, and N. A. Stanton, "Situation awareness based on eye movements in relation to the task environment," *Cognition, Technology & Work*, vol. 21, no. 1, pp. 99–111, Feb. 2019.

[18] F. Zhou, X. J. Yang, and J. C. F. De Winter, "Using Eye-Tracking Data to Predict Situation Awareness in Real Time During Takeover Transitions in Conditionally Automated Driving," *IEEE Transactions on Intelligent Transportation Systems*, vol. 23, no. 3, pp. 2284–2295, Mar. 2022.

[19] C. Lv, H. Wang, D. Cao, Y. Zhao, M. Sullman, D. J. Auger *et al.*, "A Novel Control Framework of Haptic Take-Over System for Automated Vehicles," in *2018 IEEE Intelligent Vehicles Symposium (IV)*. Changshu: IEEE, Jun. 2018, pp. 1596–1601.